Bull. Mater. Sci. (2018) 41:71
https://doi.org/10.1007/s12034-018-1600-8

Investigation of metallic nanoparticles adsorbed on the QCM sensor by SEM and AFM techniques

IOAN ALIN BUCURICA[1,2,*], ION V POPESCU[3,4], CRISTIANA RADULESCU[1,3], GHEORGHE VALERICA CIMPOCA[4], IOANA-DANIELA DULAMA[1], SOFIA TEODORESCU[1], ION VALENTIN GURGU[1] and DORIN DACIAN LET[1]

[1]Institute of Multidisciplinary Research for Science and Technology, Valahia University of Targoviste, 130004 Târgovişte, Romania
[2]Doctoral School, Faculty of Physics, University of Bucharest, 050107 Bucharest, Romania
[3]Faculty of Sciences and Arts, Valahia University of Targoviste, 130004 Târgovişte, Romania
[4]Academy of Romanian Scientists, 050094 Bucharest, Romania
*Author for correspondence (bucurica_alin@yahoo.com)

MS received 30 June 2017; accepted 28 October 2017; published online 17 May 2018

Abstract. Quartz crystal microbalance (QCM) is known as a very sensitive device used for determination of mass quantity adsorbed on sensor surface. Its detection limits are in the range of ng cm^{-2}. The adsorption mechanism of metallic nanoparticles on QCM sensor was investigated by scanning electron microscopy (SEM) and atomic force microscopy (AFM). This study aims to highlight the importance of QCM applications in nanoparticles deposition field. The layers formed through adsorption process, induced by the oscillations of the QCM sensor, were investigated by AFM for surface topography and for particle mean size values. The morphology of layers and nanoparticles dimensions were determined by SEM. For a more complex investigation of the nanoparticles adsorption mechanism, the chemical composition of layers was achieved using SEM coupled with energy dispersive X-ray spectrometer (SEM-EDS). This preliminary research involved a new approach in characterization of metallic nanoparticles layers to achieve functional assembled monolayers.

Keywords. Metallic nanoparticles; QCM; AFM; SEM; SEM-EDS.

1. Introduction

Nanoparticles are currently used in many fields, including medicine, manufacturing, materials, optical, environment, energy and electronics. The scientific interest concerning nanoparticles is given by the fact that it represents a bridge between bulk materials and atomic/molecular structures. In medical field, the nanoparticles are widely used to treat different tumours. Thus, the brain tumours and leukaemia as well can be treated using the chemotherapy drugs attached to carbon nanoparticles named nanodiamonds [1–4]. Today there is a large array of nanodiamonds for biomedical applications, especially due to their excellent optical properties and non-toxicity, as well. In other research [5], four iron-oxide nanoparticle systems were already tested as tool for targeting cancer cells. Recently, Gowda *et al* [6] have developed nanoparticles to deliver a melanoma-fighting drug directly to tumoural areas. For the growth of the bone around dental or joint implants, new nanodiamonds along with attached protein molecules were found [7–9]. The wide range of potential applications of nanoparticles continues to drive research in all fields forward. Recently, Phan *et al* [5] have exploited iron/iron oxide core/shell nanoparticle systems for nanomedicine applications due to the combination of high magnetization of the core (iron) and the chemical stability of the shell (Fe_3O_4 or γ-Fe_2O_3), which confer better properties than either material alone. Last research [10] presents new synthetic skin, an innovative composite consisted of nickel nanoparticles and polymer, which is widely used in prosthetics, demonstrating a good self-healing capability. Other researches sustain that protein-filled nanoparticles may be used in inhalable vaccines [11,12] and polymeric micelle nanoparticles were already obtained to deliver drugs to different tumours [13–15]. One of the most promising studies [16] demonstrated that cerium oxide nanoparticles act as a good antioxidant to remove the undesired oxygen free radicals present in a bloodstream of the patients, as a result of a traumatic injury. In environmental field, the most known applications of nanoparticles are the ones to clean arsenic from water wells [17], to clean-up carbon tetrachloride pollution in groundwater [18] and to destroy the volatile organic compounds (VOCs) from air (i.e., when gold nanoparticles are embedded in a porous manganese oxide to play a catalyst role) [19,20]. Recently, there was an intense interest regarding textile odour-resistants. In this respect, silver nanoparticles were used in clothing to kill bacteria [21] and zinc oxide nanoparticles were dispersed in textile coatings to protect fibres from exposure to UV rays [22–24]. Several nanoparticle

applications in energy and electronics fields are developed. Thus, the latest researches [25,26] have demonstrated that sunlight concentrated on different nanoparticles can produce steam with high energy efficiency, and the system was named solar steam device. Copper nanoparticles were used in space missions [27] and in solar cells manufacturing [28–31]. A new transistor known as a nanoparticle organic memory field-effect transistor (NOMFET) [32] was achieved. This transistor contains gold nanoparticles combined with organic molecules and can function in a similar way to synapses in the nervous system. Likewise, the palladium nanoparticles are already used in a hydrogen sensor [33,34]. Platinum–cobalt nanoparticles [35,36] as well as carbon nanoparticles [37] are being developed for fuel cells. The process of spoiling or drying out of food can be performed by using silica nanoparticles, which provide a barrier for oxygen and moisture in a plastic material used for packaging [38].

The quartz crystal microbalance (QCM) technique was used in various studies regarding the adsorption mechanism of nanoparticles on sensors [39–43]. The dynamic and dissipation modes of QCM were used to detect bacteria using gold nanoparticles [39] and to determine the mechanisms of nanoparticle monolayer formation (e.g., gold nanoparticles on poly(allylamine hydrochloride) [40], titanium dioxide nanoparticles [41], carbon-based nanoparticles [42] or gold nanoparticles [43]).

It is well known that nanoparticles in various media (i.e., gas and liquid phases) can be agglomerated (i.e., physically) and aggregated (i.e., chemically-bounded) [44]. In liquid phase (i.e., aqueous or organic), it is very difficult to obtain the homogeneous layers of nanoparticles and equivalent sizes of them. As aggregates, nanoparticles appear as clusters, which can be achieved by chemical reaction, sintering, surface growth and fragmentation. In this case, strong chemical bonds occur in clusters and the applications of these in different fields increase (e.g., catalysts, drugs, component in electronic devices, such as batteries, sensors, etc.) Between nanoparticles, agglomerations are occurring at low forces and for this reason, these can be easily destroyed by ultrasonication, stretching, fluid dispersion, or capillary condensation.

The novelty of this research is to obtain the homogeneous layers as a result of QCM oscillation frequency (5 MHz), also known as 'ultrasonic effect'. This effect prevents the massive agglomerations of nanoparticles and, at the same time, accelerates the polar solvent evaporation. Related to the scientific literature [45,46], in which different techniques were used for sensor surface improvement (e.g., non-polar organic substances), this method used sensors without supplementary organic coating, which could lead to molecular aggregates with potential risk for medical or pharmaceutical fields.

In this respect, the obtained agglomerations were characterized by two techniques: atomic force microscopy (AFM) and scanning electron microscopy (SEM). By using these analytical methods, it was possible to determine the sizes of studied nanoparticles in colloidal solutions and the shape of the agglomerations. Finally, it was observed that according to the size and nature of nanoparticles, the shape is completely different. This study involves, besides the size and shape analysis of studied nanoparticles, and a carefully layer characterization of metallic nanoparticles to achieve functional assembled monolayers, which can be used in different applications (e.g., pharmaceuticals, medicine, agriculture, food safety, electronics, etc.).

2. Materials and methods

For this study, five colloidal solutions were analysed containing metallic nanoparticles from Particular GmBH. According to certificates, the samples were electrostatically stabilized and had the following concentrations: Au (22 mg l^{-1}), Ag (17 mg l^{-1}), Pd (25 mg l^{-1}), Ti (18 mg l^{-1}) and Fe (21 mg l^{-1}). To remove the water from solutions and to achieve uniform adsorption, it was used as a QCM (QCM-200, Stanford Research Instruments) along with Ti–Pt sensors.

QCM is a very sensitive device, capable to measure mass variations in the range of ng cm^{-2} [47–51]. Sauerbrey [52] has developed an equation, which is used to correlate the frequency shift of a piezoelectric crystal with the mass variation equation (1):

$$\Delta f = -\frac{2f_0^2}{A\sqrt{\rho_q \mu_q}}\Delta m, \tag{1}$$

where Δf, frequency shift (Hz); f_0, resonant frequency (Hz; A, active crystal area (cm^2); ρ_q, density of quartz ($\rho_q = 2.648$ g cm^{-3}); μ_q, shear modulus of quartz for AT-cut crystal ($\mu_q = 2.947 \times 10^{11}$ g cm^{-1} s^{-2}); Δm, mass variation (g).

Quartz sensors covered by titanium–platinum (TiPt) layer with a frequency of 5 MHz were purchased from Stanford Research Systems. Before applying colloidal sample, the sensors were cleaned in Piranha solution, a mixture of hydrogen peroxide (30% H_2O_2, Merck) and sulphuric acid (95% H_2SO_4, Merck) with volume ratio 1:3 for 3 min. Then, sensors were immersed in deionized water (Milli-Q Water System Millipore) for 15 min and dried out in a gentle flow of nitrogen gas.

After intern calibration of QCM-200 system and resonance frequency determination of unload sensor, f_i (figure 1a) was complete, a 0.5 ml of sample was applied directly over the sensor surface in static mode. Four hours later, during which the water was removed (figure 1b), the sensor frequency, f_f was recorded and on its bases, the frequency shift was calculated.

The sensors containing adsorbed nanoparticles were investigated in first instance by NT-MDT Ntegra Prima AFM (figure 2). For topography, it was chosen at the very start, the contact AFM mode along with high resolution contact 'golden' Silicon Cantilevers CSG10, made by single crystal silicon and doped with antimony. These AFM probes are three times better than uncoated ones and the base being doped as it avoids the electrostatic charges [53,54].

Figure 1. QCM sensor (**a**) before and (**b**) after adsorption process.

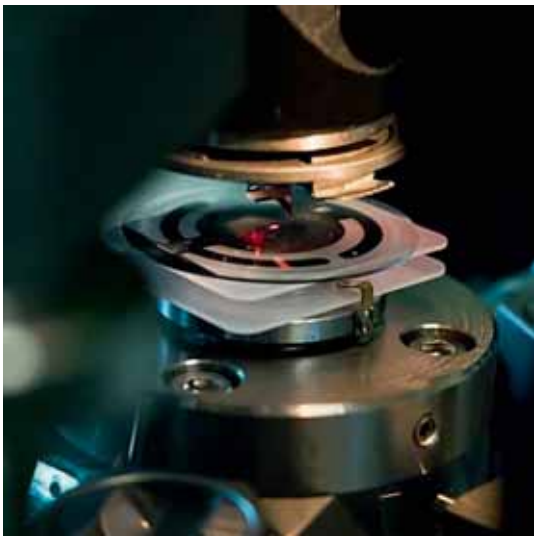

Figure 2. AFM investigation sequence.

Later on, the sensors were passed to Hitachi SU-70 SEM coupled with UltraDry energy dispersive spectrometer (EDS) by Thermo Scientific, for further analyses. The SEM is field emission (FE-SEM) type which operates under high vacuum (10^{-8} Pa), and offers 1 nm resolution at 15 kV acceleration voltage [55–58]. SEM investigations were performed under 10 kV accelerating voltage and 8–17 mm working distance range. Colloidal nanoparticles samples were also analysed using EDS to detect some possible impurities

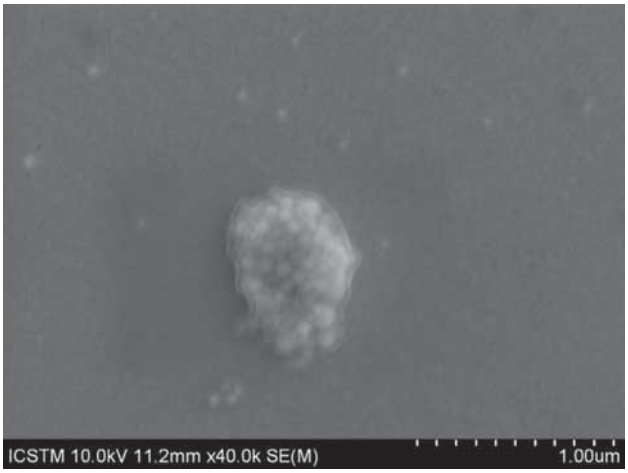

Figure 3. SEM image of Pd-agglomerated nanoparticles on thin layer.

occurred during the adsorption process of nanoparticles on the sensors.

3. Results and discussion

The nanoparticles adsorption on the QCM sensor was investigated, using five colloidal solutions (i.e., hydrocolloids). These solutions were chosen for physico-chemical characterization using complementary analytical techniques such as AFM and SEM. The morphology and topography of the

Table 1. Mass of nanoparticles adsorbed on QCM sensor surface.

	f_i (Hz)	f_f (Hz)	Δf (Hz)	C_f (Hz μg^{-1} cm^2)	Δm (μg cm^{-2})
Fe NP	5023579	5023144	−435	−56.6	7.69
Ti NP	5033900	5033529	−371		6.55
Ag NP	5027735	5027392	−343		6.06
Au NP	5025611	5025157	−454		8.02
Pd NP	5032135	5031619	−516		9.11

f_i, frequency of unload sensor; f_f, frequency of sensor after metallic nanoparticles adsorption; Δf, frequency shift ($f - f_f$); C_f, sensibility factor of the AT-cut sensor at room temperature; and Δm, mass of nanoparticles adsorbed on sensor surface.

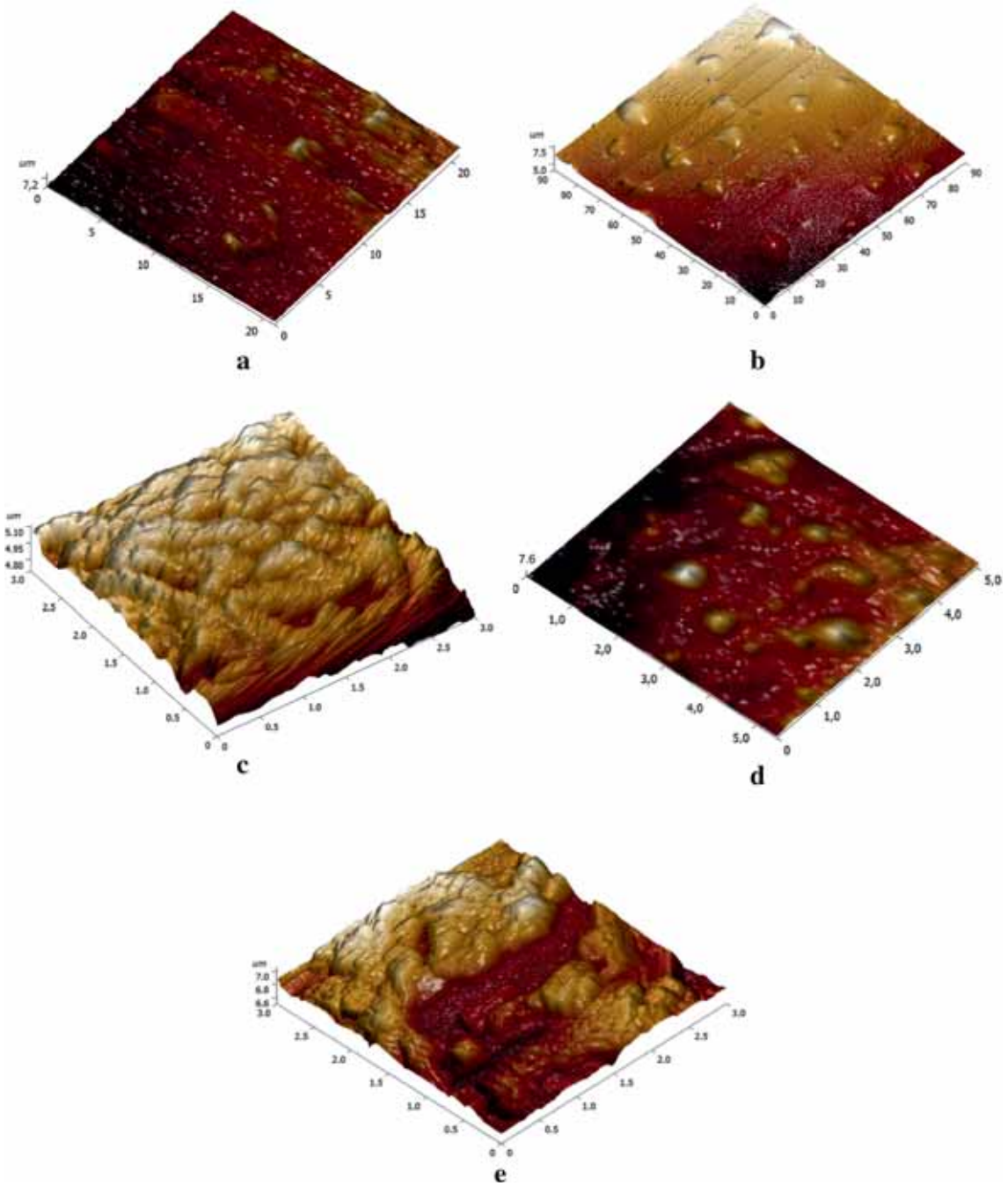

Figure 4. AFM 3D topography images for several agglomerated nanoparticles: (**a**) Ti; (**b**) Fe; (**c**) Pd; (**d**) Ag and (**e**) Au.

deposed layers were observed by both the techniques. In this respect, TiPt sensors with 1.37 cm^2 active area and 5 MHz resonant frequency were used, and thus, the Sauerbrey equation (1) is reduced to:

$$\Delta m = \Delta f / - C_{\mathrm{f}}, \tag{2}$$

where C_{f} represent the sensibility factor of the AT-cut sensor at room temperature (-56.6 Hz $\mu g^{-1} cm^2$).

Based on equation (2), the mass shift for each studied metallic nanoparticles is calculated (table 1).

All five QCM sensors showed similarities concerning adsorption mechanism. Nanoparticles were adsorbed uniformly over the entire sensor, but some investigated areas were observed with different sort of agglomerations (e.g., Pd nanoparticles, figure 3). On the layer level, these agglomerations are reduced as number, but spread on the surface of QCM sensor (figures 3–5).

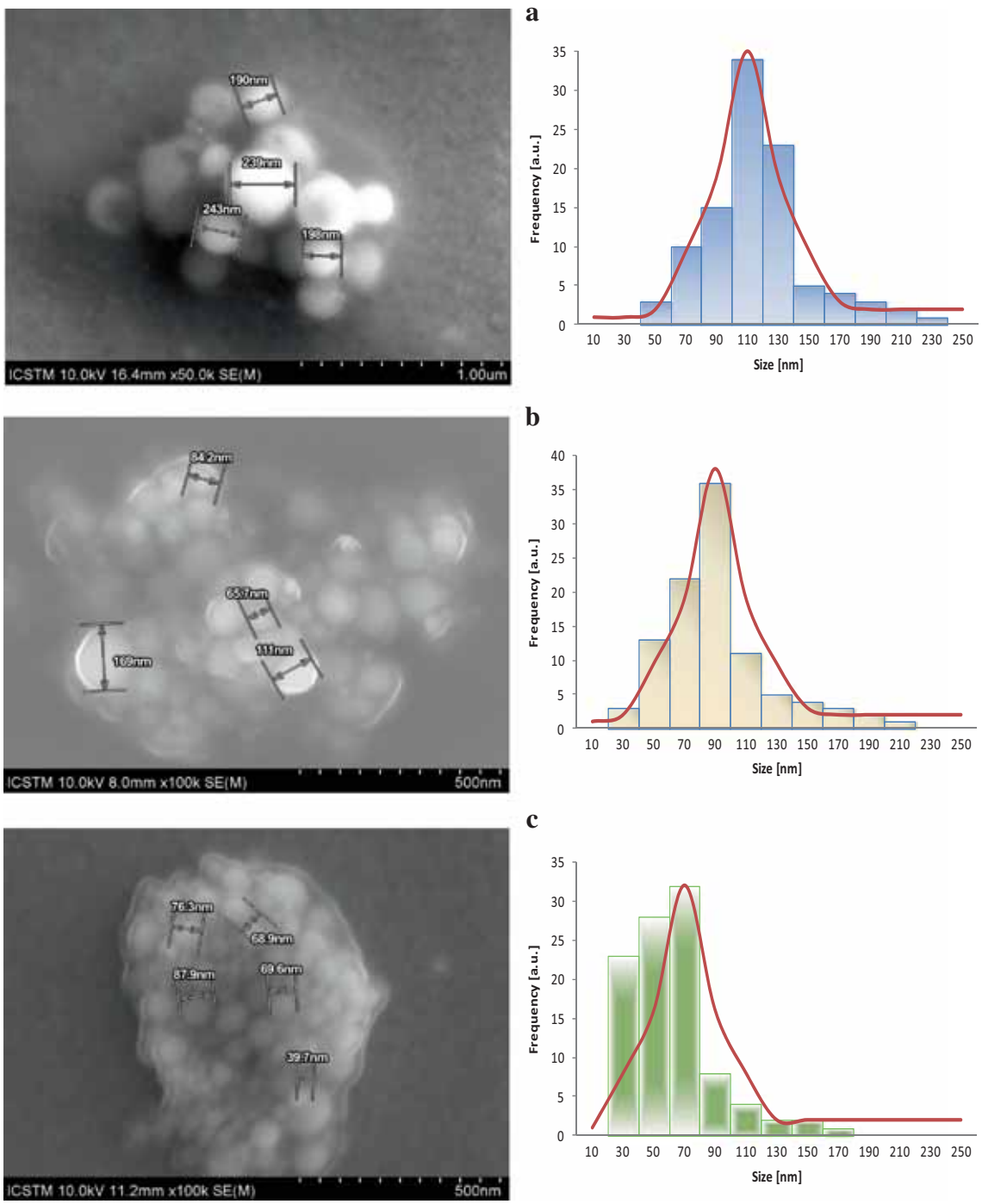

Figure 5. SEM images and size histogram of nanoparticles: (**a**) Ti; (**b**) Fe; (**c**) Pd; (**d**) Ag; and (**e**) Au.

Depending on the type and size of nanoparticles, the agglomerations show different shapes and these can be seen mainly by AFM (figure 4).

These agglomeration shapes were investigated to determine the mean size of nanoparticles. In this respect, the AFM images were processed using Nova Px software and the results were: Ti, 116 nm; Fe, 90 nm; Pd, 62 nm; Ag, 98 nm; and Au, 50 nm. These data were sustained by SEM analysis (figure 5).

The spheroid shapes of nanoparticles were clearly observed in SEM images presented in figure 5. Depending of the nature and the properties of nanoparticles, it can be concluded that the iron and palladium nanoparticles are slightly film-coated. This can be explained by the similarities between both elements (cubic structure, density, covalent radius, etc.).

Therefore, for a complex investigation of nanoparticles adsorption mechanism, the chemical composition of layers

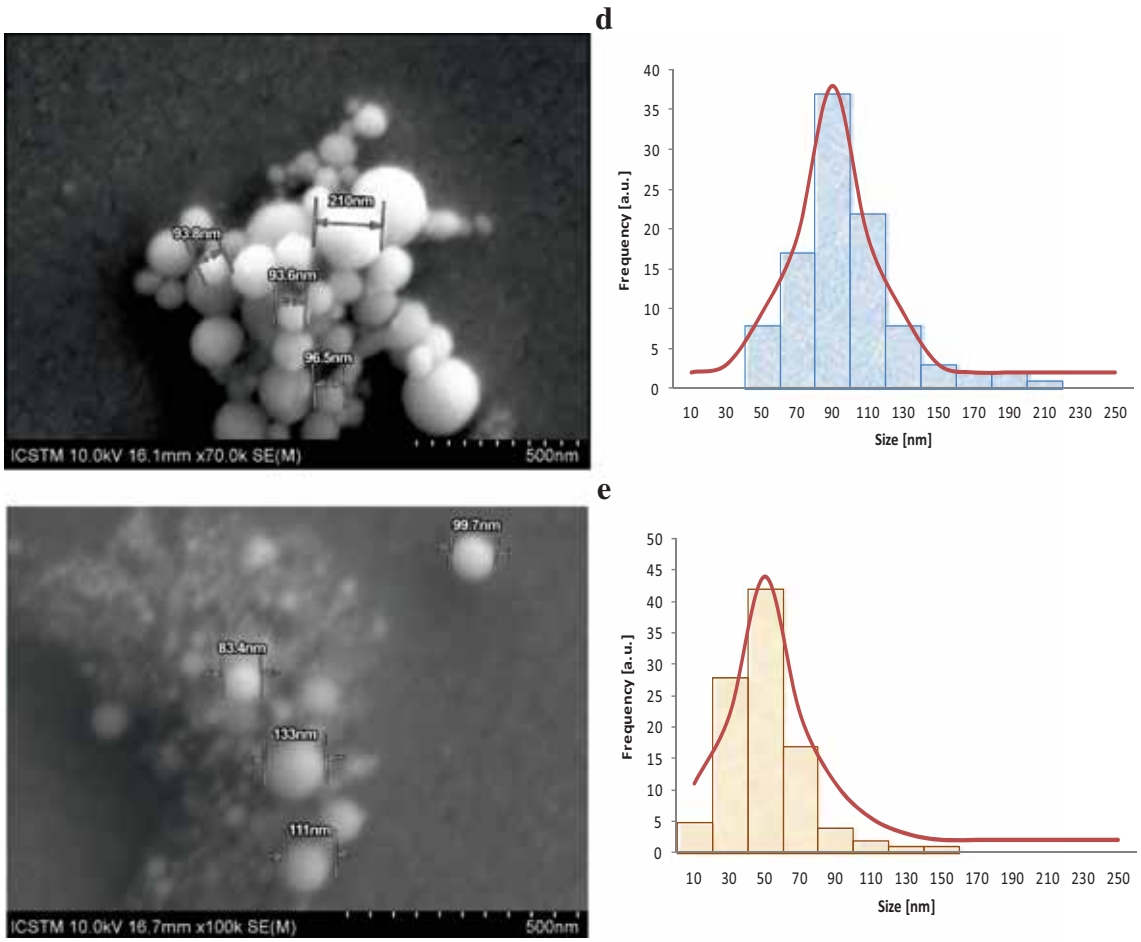

Figure 5. *Continued.*

Table 2. Elemental concentration of metallic layers determined by SEM-EDS.

	Nanoparticles				
Elements (%)	Ti NP	Fe NP	Pd NP	Ag NP	Au NP
C	13.00 ± 0.09	11.65 ± 0.24	6.80 ± 0.79	ND	10.09 ± 0.16
N	ND	ND	ND	ND	3.06 ± 0.22
O	16.91 ± 0.15	22.28 ± 0.34	8.19 ± 0.16	4.62 ± 0.12	8.57 ± 0.19
Na	3.85 ± 0.02	ND	0.45 ± 0.02	ND	2.20 ± 0.04
Si	8.71 ± 0.03	8.47 ± 0.07	14.39 ± 0.05	5.63 ± 0.05	11.45 ± 0.06
S	0.20 ± 0.03	ND	0.29 ± 0.05	ND	ND
Ti	4.53 ± 0.03	2.41 ± 0.05	3.55 ± 0.03	2.91 ± 0.05	3.25 ± 0.06
Ag	ND	ND	ND	8.19 ± 0.21	ND
Pd	ND	ND	2.29 ± 0.07	ND	ND
Fe	ND	4.83 ± 0.15	ND	ND	ND
Pt	52.72 ± 0.38	50.37 ± 1.19	64.05 ± 0.44	78.65 ± 0.34	52.88 ± 1.00
Au	ND	ND	ND	ND	8.50 ± 0.51

ND = not determined.

was achieved using SEM coupled with EDX spectrometer. The results are shown in table 2, where the concentration values for each sample can be observed.

In addition, the expected elements (Si, O from quartz crystal; Ti and Pt from sensor metallization and the nanocolloidal element) have discovered a number of other elements

such as, N, Na and S, which can appear from atmosphere during the adsorption process. In this case, the presence of these impurities (i.e., N, Na and S) can affect the quality and uniformity of the self-assembled monolayers (SAM) on these metallic surfaces. Further research will be performed and characterized few types of SAM with different application fields (e.g. pharmaceuticals, medicine, agriculture, food safety, electronics, etc.).

4. Conclusion

In this study, four techniques (QCM, AFM, SEM and EDS) were successfully combined to characterize the morphology and adsorption mechanism of different metallic nanoparticles. The main objective of this research was to obtain the nanoparticles' most uniform layers for a further manufacturing deposition processes.

Acknowledgements

We would like to thank to anonymous reviewers for their remarks and advices.

References

[1] Schrand A M, Hens S A C and Shenderova O A 2009 *Crit. Rev. Solid State Mater. Sci.* **34** 18
[2] Faklaris O, Joshi V, Irinopoulou T, Tauc P, Sennour M, Girard H *et al* 2009 *ACS Nano* **3** 3955
[3] Chow E K, Zhang X Q, Chen M, Lam R, Robinson E, Huang H *et al* 2011 *Sci. Transl. Med.* **3** 73ra21
[4] Merkel T J and DeSimone J M 2011 *Sci. Transl. Med.* **3** 73ps8
[5] Phan M H, Alonso J, Khurshid H, Lampen-Kelley P, Chandra S, Stojak Repa K *et al* 2016 *Nanomaterials* **6** 221
[6] Gowda R, Madhunapantula S V, Sharma A, Kuzu O F and Robertson G P 2014 *Mol. Cancer Ther.* **13** 2328
[7] Mochalin V N, Shenderova O, Ho D and Gogotsi Y 2011 *Nat. Nanotechnol.* **7** 11
[8] Holt K B 2007 *Philos. Trans. R Soc. A* **365** 2845
[9] Kotov N A 2010 *Science* **330** 188
[10] Correia Carabineiro S A 2017 *Molecules* **22** 857
[11] Zaffran M, Vandelaer J, Kristensen D, Melgaard B, Yadav P, Antwi-Agyei K O *et al* 2013 *Vaccine* **31** B73
[12] Chen H W, Huang C Y, Lin S Y, Fang Z S, Hsu C H, Lin J C *et al* 2016 *Biomaterials* **106** 111
[13] Popescu R C and Grumezescu A M 2015 *Curr. Top. Med. Chem.* **15** 1532
[14] Webster D M, Sundaram P and Byrne M E 2013 *Eur. J. Pharm. Biopharm.* **84** 1
[15] Hartwell B L, Antunez L, Sullivan B P, Thati S, Sestak J O and Berkland C 2015 *J. Pharm. Sci.* **104** 346
[16] Nelson B C, Johnson M E, Walker M L, Riley K R and Sims C M 2016 *Antioxidants* **5** 15
[17] Pradeep T and Anshup 2009 *Thin Solid Films* **517** 6441
[18] He F, Zhao D and Roberts C 2009 In *Nanotechnology applications for clean water* (eds) N Savage, M Diallo, J Duncan, A Street and R Sustich (USA: William Andrew Publication)
[19] Cao G 2004 *Nanostructures and nanomaterials: synthesis, properties and applications* (London: Imperial College Press)
[20] Feldheim D L and Foss Jr C A 2002 *Metal nanoparticles: synthesis characterization and applications* (New York: Marcel Dekker Inc.)
[21] Hipler (Jena) U C and Jena E P 2006 *Biofunctional textiles and the skin* (Basel: Karger AG)
[22] Kathirvelu S, D'Souza L and Dhurai B 2009 *Indian J. Fibre Text.* **34** 267
[23] Radulescu C, Hossu A M, Manea L and Tarabasanu-Mihaila C 2007 *Rev. Chim. (Bucharest)* **58** 958
[24] Radulescu C, Ionita I, Moater E I and Gheboianu A 2010 *Ind. Text.* **61** 168
[25] Chen C, Li Y, Song J, Yang Z, Kuang Y, Hitz E *et al* 2017 *Adv. Mater.* **2017** 1701756
[26] Mane S G, Sawant P R and Shinde N N 2015 *Int. Res. J. Eng. Tech.* **2** 703
[27] Gawande M B, Goswami A, Felpin F X, Asefa T, Huang X, Silva R *et al* 2016 *Chem. Rev.* **116** 3722
[28] Gawande M B, Shelke S N, Zboril R and Varma R S 2014 *Acc. Chem. Res.* **47** 1338
[29] Li G, Li X H and Zhang Z J 2011 *Prog. Chem.* **23** 1644
[30] Yin G, Nishikawa M, Nosaka Y, Srinivasan N, Atarashi D, Sakai E *et al* 2015 *ACS Nano* **9** 2111
[31] Bhanushali S, Ghosh P, Ganesh A and Cheng W 2015 *Small* **11** 1232
[32] Bichler O, Zhao W, Alibart F, Pleutin S, Vuillaume D and Gamrat C 2010 *IEEE Trans. Electron Dev.* **57** 3115
[33] Noh J S, Lee J M and Lee W 2011 *Sensors* **11** 825
[34] Hung C, Lin H, Chen H, Tsai Y, Lai P, Fu S *et al* 2007 *Sens. Actuat. B* **122** 81
[35] Wang G H, Hilgert J, Richter F H, Wang F, Bongard H J, Spliethoff B *et al* 2014 *Nat. Mater.* **13** 293
[36] Bauer J C, Chen X, Liu Q S, Phan T H and Schaak R E 2008 *J. Mater. Chem.* **18** 275
[37] Tan C W, Tan K H, Ong Y T, Mohamed A R, Hussein S, Zein S *et al* 2011 In *Environmental chemistry for a sustainable world* (eds) E Lichrfouse, J Schwarzbauer and D Robert (Dordrecht–Heidelberg–London–New York: Springer)
[38] Martirosyan A and Schneider Y J 2014 *Int. J. Environ. Res. Public Health* **11** 5720
[39] Masdor N A, Altintas Z and Tothill I E 2016 *Biosens. Bioelectron.* **78** 328
[40] Maciejewska-Prończuk J, Morga M, Adamczyk Z, Oćwieja M and Zimowska M 2017 *Colloids Surf. A* **514** 226
[41] Kananizadeh N, Rice C, Lee J, Rodenhausen K B, Sekora D, Schubert Mathias *et al* 2017 *J. Hazard. Mater.* **322** 118
[42] Chen Q, Xu S, Liu Q, Masliyah J and Xu Z 2016 *Adv. Colloid Interface Sci.* **233** 94
[43] Bailey C M, Kamaloo E, Waterman K L, Wang K F, Nagarajan R and Camesano T A 2015 *Biophys. Chem.* **203–204** 51
[44] Eggersdorfer M L and Pratsinis S E 2014 *Adv. Powder Technol.* **25** 71
[45] Jiang J, Oberdörster G and Biswas P 2009 *J. Nanopart. Res.* **11** 77
[46] Reimhult K, Yoshimatsu K, Risveden K, Chena S, Ye L, Krozera A 2008 *Biosens. Bioelectron*. **23** 1908

[47] Cimpoca G V, Radulescu C, Dulama I D, Popescu I V, Stihi C, Gheboianu A *et al* 2009 *AIP Conf. Proc.* **1203** 409
[48] Cimpoca G V, Radulescu C, Dulama I D, Popescu I V, Gheboianu A, Bancuta I *et al* 2009 *AIP Conf. Proc.* **1203** 160
[49] Cimpoca G V, Radulescu C, Popescu I V, Dulama I D, Ionita, I, Cimpoca M *et al* 2009 *AIP Conf. Proc.* **1203** 415
[50] Cimpoca G V, Popescu I V, Dulama I D, Radulescu C, Bancuta I, Cimpoca M *et al* 2009 *IEEE Proc. CAS Conf.* **1–2** 135
[51] Dulama I D, Popescu I V, Cimpoca G V, Radulescu C, Bucurica I A, Let D *et al* 2013 *IEEE Proc. CAS Conf.* **1–2** 107
[52] Sauerbrey G 1959 *Z. Phys.* **155** 206
[53] Long C J and Cannara R J 2015 *Rev. Sci. Instrum.* **86** 073703
[54] Let D, Bucurica A, Dulama I, Bacinschi Z, Mihai S and Filip V 2015 *Sci. Bull. Mater. Mech.* **10** 71
[55] Negrea A, Bacinschi Z, Bucurica I A, Teodorescu S and Stirbescu R 2016 *Rom. J. Phys.* **61** 527
[56] Radulescu C, Stihi C, Popescu I V, Varaticeanu B, Telipan G, Bumbac M *et al* 2016 *J. Sci. Arts* **1** 77
[57] Teodorescu S, Ion R M, Nechifor G, Bucurica I A, Dulama I D, Stirbescu R M *et al* 2017 *Rev. Chim. (Bucharest)* **68** 869
[58] Bintintan A, Gligor M, Dulama I D, Teodorescu S, Stirbescu R M and Radulescu C 2017 *Rev. Chim. (Bucharest)* **68** 847